J|A|C|S COMMUNICATIONS

Published on Web 02/24/2004

The Origin of Sticking between a Hydroperoxy Radical and a Water Surface

Stephen D. Belair, Heriberto Hernandez, and Joseph S. Francisco*

Department of Chemistry and Department of Earth and Atmospheric Science, Purdue University, West Lafayette, Indiana 47907-2084

Received October 29, 2003; E-mail: francisc@purdue.edu

An understanding of how gas-phase radicals in the earth's atmosphere become incorporated with cloud droplets or aerosols is a vital part of understanding the chemical budgeting of these highly reactive species. The hydroperoxy radical (HO_2) is a major species in the HO_X chemical family.[1] A number of field observations[2−4] have reported gas-phase HO_2 concentrations in the atmosphere, but these measurements have been found to disagree with atmospheric model predictions. Heterogeneous uptake of HO_2 has been considered to explain the discrepancy. However, laboratory studies[5,6] of the uptake of HO_2 by water have shown, with considerable uncertainty, that little HO_2 is accommodated. A recent theoretical study showed that the HO_2 radical had an affinity for binding to a water surface;[7,8] however, it is not clear what gives rise to the unusual binding of HO_2 to one water molecule. Moreover, the same interactions may not account for the special characteristics of the binding between HO_2 and a water surface. In this letter, we report on the origin of the sticking of an HO_2 radical to a water surface.

An $(H_2O)_{20}$ spherical cage is used as a model of a cloud droplet.[7] This model was chosen because it is the perfect balance between being large enough to contain an HO_2 radical and small enough for quantum chemistry optimizations. Three stable configurations of $HO_2{\cdot}(H_2O)_{20}$ were reported previously.[7] The most stable of these is shown in Figure 1a. In this study, to gain further insight into the bonding between an HO_2 radical and a water surface, we further examine the $HO_2{\cdot}(H_2O)_{20}$ structure by performing a natural bond orbital[9] (NBO) analysis of it, as well as two- and six-water substructures taken directly from the fully optimized $HO_2{\cdot}(H_2O)_{20}$. $HO_2{\cdot}(H_2O)_2$ was made up of the radical and the two nearest water molecules. It is shown in Figure 1b. $HO_2{\cdot}(H_2O)_6$ was made up of the $HO_2{\cdot}(H_2O)_2$ structure plus the four other water molecules to which those two waters were hydrogen bound. The $HO_2{\cdot}(H_2O)_{20}$ structure from the previous study[7] was optimized using the Hartree−Fock and B3LYP methods and a 6-31G(d) basis set. The NBO calculations performed in the present work were done at the same levels of theory. All quantum chemistry calculations were performed using Gaussian 98[10] and NBO 5.0.[11]

The $HO_2{\cdot}H_2O$ structure has been described previously as a five-membered ring with one of the hydrogens of the water tilted out of the plane.[8] This structure can be constructed from the one in Figure 1b by removing the lower water molecule and allowing O(3) and H(5) to become adjacent members of the ring. The NBO analysis of this complex revealed that its intermolecular attraction consisted of five significant contributions, four of which are due to transfers of electron density in the $H_2O \rightarrow HO_2$ direction. The following results are summarized in Table 1 where the energies of the significant interactions are reported. The largest contribution is due to a $n \rightarrow \sigma^*$ transfer, where the lone pair is from the oxygen of the water and the σ antibonding orbital is from the HO bond of the radical. This interaction energy is 16.3 kcal mol^{-1}. A second significant contribution is the $\sigma \rightarrow \sigma^*$ from the OH bond of the radical to the "in-ring" OH bond of the water. There was found to be no significant interaction between the terminal oxygen of the radical and the "in-ring" hydrogen of the water. This lends new insight to the previous results that suggested that there was a second hydrogen bond between those two atoms.[8] The present calculations reveal that the orientation which appears to be due to a second hydrogen bond is actually due to the weaker secondary interaction from the $\sigma_{O(4)H(5)} \rightarrow \sigma_{O(1)H(2)}^*$ transition.

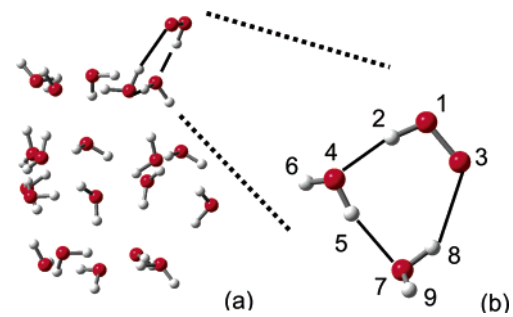

Figure 1. Fully optimized geometry of $HO_2{\cdot}(H_2O)_{20}$. (a) Relative orientation of the HO_2 radical to the $(H_2O)_{20}$ cage. (b) Expanded view of the HO_2 radical and the two water molecules to which it is hydrogen bound.

The NBO analysis of $HO_2{\cdot}(H_2O)_2$ revealed that, as in the $HO_2{\cdot}H_2O$ case, both $n \rightarrow \sigma^*$ and $\sigma \rightarrow \sigma^*$ interactions occur. In the following text, the symbols ′ and ″ are used to distinguish between different lone pairs on the same oxygen atom, RY denotes Rydberg, and CR denotes core. By far, the largest contributions are due to $n \rightarrow \sigma^*$ transitions, where the strengths of the $n_{O(4)}'' \rightarrow \sigma_{O(1)H(2)}^*$, $n_{O(7)}'' \rightarrow \sigma_{O(4)H(5)}^*$, $n_{O(3)}'' \rightarrow \sigma_{O(7)H(8)}^*$, and $n_{O(3)}' \rightarrow \sigma_{O(7)H(8)}^*$ are 21.9, 15.6, 2.7, and 1.9 kcal mol^{-1}, respectively. $\sigma \rightarrow RY^*$ and $CR \rightarrow \sigma^*$ interactions also contribute to the intermolecular attraction. One major difference between the $HO_2{\cdot}H_2O$ and $HO_2{\cdot}(H_2O)_2$ cases is that the $HO_2{\cdot}(H_2O)_2$ case has an attractive component that involves the terminal oxygen of the radical O(3). Interaction with O(3) is possible in this case because of the larger, more relaxed, hydrogen bonding angle.

Similarly, the $n \rightarrow \sigma^*$ interactions are also the strongest for the $HO_2{\cdot}(H_2O)_2$ portions of $HO_2{\cdot}(H_2O)_6$ and $HO_2{\cdot}(H_2O)_{20}$. By looking at the total columns in Table 1, it can be seen that the differences in total interaction energies between the radical and each nearest-neighbor water molecule, for increasingly larger water clusters, are generally small. The most effected water/radical interaction is $n_{O(4)}'' \rightarrow \sigma_{O(1)H(2)}^*$ which increases by 0.2 kcal mol^{-1} (out of ∼22 kcal/mol) when increasing from 2 to 6 waters. This suggests that the binding of the radical to the water cluster is a local phenomenon.

In Figure 2, we present a 3-D plot[12] showing the $\sigma_{O(4)H(5)} \rightarrow \sigma_{O(1)H(2)}^*$ and $n_{O(3)} \rightarrow \sigma_{O(7)H(8)}^*$ interactions between the HO_2 radical and the water dimer. The figure also suggests, by demonstrating the diffuseness of the $\sigma_{O(1)H(2)}^*$ orbital, that the $CR_{O(4)} \rightarrow \sigma_{O(1)H(2)}^*$ interaction is also a source of the binding between the radical and the water. This is confirmed by the data in Table 1.

10.1021/ja030604d CCC: $27.50

Table 1. Interaction Energies (kcal/mol)[a]

	$HO_2{\cdot}H_2O$			$HO_2{\cdot}(H_2O)_2$			$HO_2{\cdot}(H_2O)_6$			$HO_2{\cdot}(H_2O)_{20}$		
	α	β	total	α	β	total	α	β	total	α	β	total
$\sigma_{O(1)O(3)} \rightarrow RY_{O(4)}^*$	0.07	0.05	0.12	0.13	0.10	0.23	0.14	0.11	0.25	0.14	0.11	0.25
$n_{O(3)}' \rightarrow \sigma_{O(7)H(8)}^*$				1.02	0.84	1.86	1.03	0.82	1.85	1.04	0.84	1.88
$n_{O(3)}'' \rightarrow \sigma_{O(7)H(8)}^*$				0.90	1.77	2.67	0.94	1.85	2.79	0.92	1.81	2.73
$\sigma_{O(4)H(5)} \rightarrow \sigma_{O(1)H(2)}^*$	0.19	0.19	0.38	0.37	0.37	0.74	0.36	0.35	0.71	0.36	0.35	0.71
$CR_{O(4)} \rightarrow \sigma_{O(1)H(2)}^*$	0.09	0.09	0.18	0.13	0.13	0.26	0.13	0.13	0.26	0.13	0.13	0.26
$n_{O(4)}' \rightarrow \sigma_{O(1)H(2)}^*$	0.04	0.04	0.08	0.10	0.09	0.19	0.10	0.10	0.20	0.11	0.11	0.22
$n_{O(4)}'' \rightarrow \sigma_{O(1)H(2)}^*$	8.19	8.09	16.28	11.04	10.88	21.92	11.16	11.00	22.16	11.10	10.94	22.04
$\sigma_{O(7)H(8)} \rightarrow \sigma_{O(4)H(5)}^*$				0.28	0.28	0.56	0.28	0.28	0.56	0.29	0.29	0.58
$CR_{O(7)} \rightarrow \sigma_{O(4)H(5)}^*$				0.08	0.08	0.16	0.08	0.08	0.16	0.08	0.08	0.16
$n_{O(7)}' \rightarrow \sigma_{O(4)H(5)}^*$				0.06	0.06	0.12	0.48	0.48	0.96	0.39	0.39	0.78
$n_{O(7)}' \rightarrow \sigma_{O(4)H(5)}^*$				7.79	7.79	15.58	6.97	6.96	13.93	7.17	7.16	14.33

[a] σ = covalent bond, n = lone pair, CR = core pair, RY = Rydberg orbital, * = antibonding, ′ and ″ denote different lone pairs, α and β denote the majority and minority spins, and "total" is the sum α + β.

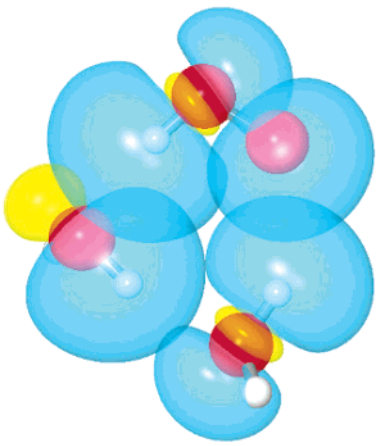

Figure 2. Graphic representation of the relevant natural bond orbitals of $HO_2{\cdot}(H_2O)_2$. The orbitals shown are: $\sigma_{O(1)H(2)}^*$, $n_{O(3)}$, $\sigma_{O(4)H(5)}$, $\sigma_{O(7)H(8)}^*$. (The numeric labels for the atoms are given in Figure 1.)

Bond orders were calculated using natural resonance theory.[11] First, an analysis was performed on each monomer unit. Comparison of the monomer data to that of $HO_2{\cdot}(H_2O)_2$ reveals that both of the covalent bonds of the radical are weakened upon complexation: the bond orders of the O(1)H(2) and O(1)O(3) bonds are weakened from 0.9923 and 1.5047 to 0.9802 and 1.5026, respectively. Additionally, those covalent HO bonds within the water molecules that have their hydrogens participating in hydrogen bonds are also weakened due to complexation. The weakening of the O(1)O(3) bond is consistent with the data from Table 1 that show $\sigma_{O(1)O(3)} \rightarrow RY_{O(4)}^*$ as a contribution to the binding, and the weakening of the O(1)H(2) bond is explained by the fact that there are four different sources of electron density transferred into the $\sigma_{O(1)H(2)}^*$ orbital. These findings are significant for a complete understanding of HO_2 chemistry because most chemical reactions involving HO_2 will require the breaking of one or both of its covalent bonds.

Through this study, we have found that the interaction of an HO_2 radical with a water surface can be described with a localized interaction picture. The interaction is not greatly influenced by increasing the number of water molecules from 2 to 20. In the case of HO_2 interacting with a water surface, our analysis shows that the origin of the bonding of HO_2 to the water surface is largely due to $n \rightarrow \sigma^*$ interactions. The two significant sources of this are orbital overlap between (1) a nonbonding lone pair from the water molecule that is bound to the hydrogen of the HO_2 and the σ^*_{OH} antibonding orbital of the HO_2 radical and (2) nonbonding electron density of the terminal oxygen of the HO_2 and the "in-ring" σ^*_{OH} antibonding orbital of the other water molecule. These interactions are the major forces that account for the sticking of HO_2 to a water surface.

It has been the general assumption that very few collisional interactions between radicals and water molecules result in chemical reactions and/or strongly bound complexes.[13,14] The hydroperoxy radical is the only known radical that has such strong interactions with water. Identifying the fundamental interactions that govern the sticking between the HO_2 radical and a water surface and realizing the local nature of this phenomenon are significant. It is now possible to use these essential underlying properties to identify other radical species that have strong binding interactions with water surfaces and aerosols and whose chemistry might be affected by the presence of saturated water vapor, clouds, and aerosols.

References

(1) Finlayson-Pitts, B. J.; Pitts, J. N., Jr. *Chemistry of the Upper and Lower Atmosphere*; Academic Press: San Diego, 2000.
(2) Cantrell, C. A.; Shetter, R. E.; Gilpin, T. M.; Calvert, J G.; Eisele, F. L.; Tanner, D. J. *J. Geophys. Res.* **1996**, *101*, 14653.
(3) Carslaw, N.; Creasey, D. J.; Heard, D. E.; Lewis, A. C.; McQuaid, J. B.; Pilling, M. J.; Monks, P. S.; Bandy, B. J.; Penkett, S. A. *J. Geophys. Res.* **1999**, *104*, 30241.
(4) Kanaya, Y.; Sadanaga, Y.; Matsumoto, J.; Sharma, U. K.; Hirokawa, J.; Kajii, Y.; Akimoto, H. *J. Geophys. Res.* **2000**, *105*, 24205.
(5) Mozurkewich, M.; McMurry, P. H.; Gupta, A.; Calvert, J. G. *J. Geophys. Res.* **1987**, *92*, 4163.
(6) Hanson, D. R.; Burkholder, J. B.; Howard, C. J.; Ravishankara, A. R. *J. Phys. Chem.* **1992**, *96*, 4979.
(7) Shi, Q.; Belair, S. D.; Francisco, J. S.; Kais, S. *Proc. Natl. Acad. Sci. U.S.A.* **2003**, *100*, 9686.
(8) Aloisio, S.; Francisco, J. S. *J. Phys. Chem. A* **1998**, *102*, 1899.
(9) Foster, J. P.; Weinhold, F. *J. Am. Chem. Soc.* **1980**, *102*, 7211.
(10) Frisch, M. J.; Trucks, G. W.; Schlegel, H. B.; Scuseria, G. E.; Robb, M. A.; Cheeseman, J. R.; Zakrzewski, V. G.; Montgomery, J. A., Jr.; Stratmann, R. E.; Burant, J. C.; Dapprich, S.; Millam, J. M.; Daniels, A. D.; Kudin, K. N.; Strain, M. C.; Farkas, O.; Tomasi, J.; Barone, V.; Cossi, M.; Cammi, R.; Mennucci, B.; Pomelli, C.; Adamo, C.; Clifford, S.; Ochterski, J.; Petersson, G. A.; Ayala, P. Y.; Cui, Q.; Morokuma, K.; Malick, D. K.; Rabuck, A. D.; Raghavachari, K.; Foresman, J. B.; Cioslowski, J.; Ortiz, J. V.; Baboul, A. G.; Stefanov, B. B.; Liu, G.; Liashenko, A.; Piskorz, P.; Komaromi, I.; Gomperts, R.; Martin, R. L.; Fox, D. J.; Keith, T.; Al-Laham, M. A.; Peng, C. Y.; Nanayakkara, A.; Challacombe, M.; Gill, P. M. W.; Johnson, B.; Chen, W.; Wong, M. W.; Andres, J. L.; Gonzalez, C.; Head-Gordon, M.; Replogle, E. S.; Pople, J. A. *Gaussian 98*, revision A.9; Gaussian, Inc.: Pittsburgh, PA, 1998.
(11) Glendening, E. D.; Badenhoop, J. K.; Reed, A. E.; Carpenter, J. E.; Bohmann, J. A.; Morales, C. M.; Weinhold, F. *NBO 5.0*; Theoretical Chemistry Institute, University of Wisconson, Madison: Madison, WI, 2001.
(12) Wendt, M.; Weinhold, F. *NBOView 1.0*; Theoretical Chemistry Institute, University of Wisconsin, Madison: Madison, WI, 2001.
(13) Chemical Kinetics and Photochemical Data for Use in Atmospheric Studies, Jet Propulsion Laboratory, California Institute of Technology, Pasadena CA, Evaluation 14, 2003.
(14) Cox, R. A. *Chem. Rev.* **2003**, *103*, 4533.

JA030604D